Quasi-thermal noise in space plasma: "kappa" distributions

G. Le Chat,[1] K. Issautier,[1] N. Meyer-Vernet,[1] I. Zouganelis,[2] M. Maksimovic,[1] and M. Moncuquet[1]
[1]*LESIA, Observatoire de Paris, CNRS, UPMC, Université Paris Diderot, 5 Place Jules Janssen, 92195 Meudon, France*
[2]*Laboratoire de Physique des Plasmas, UPMC, Ecole Polytechnique, CNRS, Univ. Paris 11, 4 avenue de Neptune, 94107 Saint-Maur-des-Fossés, France*

(Received 15 July 2009; accepted 14 September 2009; published online 9 October 2009)

The transport of energy in collisionless plasmas, especially in space plasmas, is far from being understood. Measuring the temperature of the electrons and their nonthermal properties can give important clues to understand the transport properties. Quasi-thermal noise (QTN) spectroscopy is a reliable tool for measuring accurately the electron density and temperature since it is less sensitive to the spacecraft perturbations than particle detectors. This work models the plasma QTN using a generalized Lorentzian ("kappa") distribution function for the electrons. This noise is produced by the quasi-thermal fluctuations of the electrons and by the Doppler-shifted thermal fluctuations of the ions. A sum of two Maxwellian functions has mainly been used for modeling the QTN of the electrons, but the observations have shown that the electrons are better fitted by a kappa distribution function. Pioneer work on QTN calculation only considered integer values of κ. This paper extends these calculations to real values of κ and gives the analytic expressions and numerical calculations of the QTN with a kappa distribution function. This paper shows some generic properties and gives some practical consequences for plasma wave measurements in space. © *2009 American Institute of Physics*. [doi:10.1063/1.3243495]

I. INTRODUCTION

In collisionless plasma, like the solar wind, the mechanism of energy transport is still an open question. Due to the high difference of mass between the ions and the electrons, the electrons transport the energy whereas the ions transport the impulsion. Consequently, measuring accurately the temperature of the electrons and their nonthermal properties with quasi-thermal spectroscopy can give important clues to understand the energy transport properties.

By the same way as a passive electric antenna is sensitive to electromagnetic waves, it is also sensitive to local fluctuations of the electric potential. These fluctuations are produced by the motions of the ambient electrons and ions. As soon as the plasma is stable, this quasi-thermal noise (QTN) is completely determined by the particle velocity distributions in the frame of the antenna.[1]

The problem is simpler in the absence of a static magnetic field or at frequencies much higher than the electron gyrofrequency, since in this case the plasma can be considered to be an assembly of "dressed test" particles moving in straight lines. The QTN spectrum around the plasma frequency f_p consists of a noise peak just above f_p produced by electron quasi-thermal fluctuations. Since the plasma density n_e is proportional to f_p^2, this allows an accurate measurement of the electron density. In addition, since the shape of the spectrum is determined by the electron velocity distribution, the analysis of the spectrum reveals its properties. One of the main advantages of the QTN spectroscopy is its relative immunity to the spacecraft potential and photoelectrons perturbations which, in general, affect particle analyzers.[2,3]

A sum of two Maxwellian functions has mainly been used for modeling the electron velocity distributions. The observations have shown that the suprathermal electrons are better fitted by a generalized Lorentzian ("kappa") distribution function,[4] first introduced to model space data by Vasyliunas[5] and Olbert.[6] In this paper, we compute the QTN obtained for such electron distribution functions with real kappa parameter. Chateau and Meyer-Vernet[7] only considered integer values of κ in order to simplify the calculation of the longitudinal dielectric permittivity. Section II shows how to generalize this calculation to real values of kappa and gives the corresponding QTN. In Sec. III, we present other contributions to the thermal noise in usual space plasmas. General properties of the QTN are shown in Sec. IV.

II. KAPPA ELECTRON THERMAL NOISE

A. Basics

The voltage power spectrum of the plasma QTN at the terminals of an antenna in a plasma drifting with velocity $\vec{V}$ is

$$V_\omega^2 = \frac{2}{(2\pi)^3}\int \left|\frac{\vec{k}\cdot\vec{J}}{k}\right|^2 E^2(\vec{k},\omega-\vec{k}\cdot\vec{V})d^3k. \quad (1)$$

The first term in the integral involves the antenna response to electrostatic waves, which depends on the Fourier transform $\vec{J}(\vec{k})$ of the current distribution along the antenna. The second term is the autocorrelation function of the electrostatic field fluctuations in the antenna frame. At frequencies much higher than the gyrofrequency, we have

$$E^2(\vec{k},\omega) = 2\pi \frac{\Sigma_j q_j^2 \int f_i(\vec{v})\,\delta(\omega - \vec{k}\cdot\vec{v})d^3v}{k^2\varepsilon_0^2|\varepsilon_L(\vec{k},\omega)|^2}, \tag{2}$$

$f_j(\vec{v})$ being the velocity distribution of the jth species of charge q_j and $\varepsilon_L(\vec{k},\omega)$ the plasma longitudinal function.[8]

In the case of electrons, the thermal velocity is usually higher than the plasma velocity $\vec{V}$, so using a few manipulations using the isotropy of $f(\vec{v})$,[9,10] we obtain

$$V^2 = \frac{16m\omega_p^2}{\pi\varepsilon_0}\int_0^\infty \frac{F(kL)B(k)}{k^2|\varepsilon_L|^2}dk \tag{3}$$

with

$$B(k) = \frac{2\pi}{k}\int_{\omega/k}^\infty vf(v)dv, \tag{4}$$

$$\varepsilon_L = 1 + \frac{2\pi\omega_p^2}{k}\int_{-\infty}^{+\infty} \frac{v_\parallel f(v_\parallel)}{kv_\parallel - \omega - io}dv_\parallel, \tag{5}$$

where $v_\parallel$ is the component of $\vec{v}$ parallel to $\vec{k}$. The term io denotes an infinitesimal positive imaginary part, and the function F specifies the antenna geometry as

$$F(x) = \frac{1}{x}\left[\mathrm{Si}(x) - \frac{1}{2}\mathrm{Si}(2x) - \frac{2}{x}\sin^4\left(\frac{x}{2}\right)\right] \quad \text{(wires)}, \tag{6}$$

$$F(x) = \frac{1}{4}\left(1 - \frac{\sin x}{x}\right) \quad \text{(spheres)}, \tag{7}$$

where Si is the sine integral function.

B. Choice of the distribution function

We choose the following generalized Lorentzian function as electron velocity distribution:

$$f_\kappa(v) = \frac{A}{(1 + v^2/\kappa v_0^2)^{\kappa+1}}, \tag{8}$$

with

$$A = \frac{\Gamma(\kappa+1)}{(\pi\kappa)^{3/2}v_0^3\Gamma(\kappa-1/2)}, \tag{9}$$

where $\Gamma(x)$ denotes the gamma function and v_0 is the thermal speed related to the kinetic temperature T_e as

$$v_0 = \sqrt{\frac{2\kappa-3}{\kappa}\frac{k_BT_e}{m_e}}, \tag{10}$$

where k_B is the Boltzmann constant and m_e is the electron mass.

Such f_κ functions will be named in this paper as "kappa functions;" κ is a real number, which, from Eq. (10), must be greater than 3/2. In the upper limit $\kappa\to\infty$, these functions are equivalent to Maxwellian functions.

These functions were largely discussed in Refs. 7 and 11 and citations therein. As pointed out by Valentini and D'Agosta,[12] the interest of kappa distributions to describe experimental data is increased since these distributions turn out to be a consequence of the entropy generalization through the generalized Boltzmann H theorem[13–17] in the debated nonextensive thermodynamics proposed by Tsallis in 1988.[18] Furthermore, related distribution functions are reproduced from the Fokker–Planck equation as a consequence of wave-particle interactions in the presence of collisions and are compatible with the Kullback relative entropy.[19]

We define the Debye length in this plasma as

$$L_D = \frac{v_0}{\omega_p}\left(\frac{\kappa}{2\kappa-1}\right)^{1/2}, \tag{11}$$

which is the shielding distance of low-frequency electric perturbations with a kappa distribution.[7]

C. Longitudinal dielectric permittivity

The longitudinal dielectric permittivity is given by Eq. (5). Considering a kappa function, we obtain

$$\varepsilon_L = 1 + \frac{2\pi\omega_p^2}{k}A\int_{-\infty}^{+\infty}\frac{v_\parallel}{(kv_\parallel - \omega - io)(1 + v_\parallel^2/\kappa v_0^2)^{\kappa+1}}dv_\parallel. \tag{12}$$

Setting $x = v_\parallel/\kappa^{1/2}v_0$ and $z = \omega/\kappa^{1/2}kv_0$, and using partial fraction decomposition of the integrand, we obtain

$$\varepsilon_L = 1 + \frac{2\pi\omega_p^2}{k^2}\left(\frac{1}{\pi v_0^2}\frac{\kappa-1/2}{\kappa} + zI\right) \tag{13}$$

with

$$I = Av_0\kappa^{1/2}\int_{-\infty}^{+\infty}\frac{dx}{(x - z - io)(x^2+1)^{\kappa+1}}. \tag{14}$$

The integrand I shows a pole for $x = z + io$. Setting

$$\frac{1}{(x^2+1)^{\kappa+1}} = \left[\frac{1}{(x^2+1)^{\kappa+1}} - \frac{1}{(z^2+1)^{\kappa+1}}\right] + \frac{1}{(z^2+1)^{\kappa+1}}, \tag{15}$$

we obtain

$$I = Av_0\kappa^{1/2}\left\{\int_{-\infty}^{+\infty}\frac{1}{(x-z-io)}\left[\frac{1}{(x^2+1)^{\kappa+1}} - \frac{1}{(z^2+1)^{\kappa+1}}\right]dx + \left[\frac{1}{(z^2+1)^{\kappa+1}}\int_{-\infty}^{+\infty}\frac{dx}{(x-z-io)}\right]\right\}. \tag{16}$$

The first integrand shows a multiplying factor that vanishes when $x = z$. It is analytic near the real axis and the term io is no longer required. The second term is calculated by the residue theorem, indenting the contour about $z + io$ with a small semicircle and closing it by a large semicircle in the upper half-plane, and gives

$$\frac{i\pi}{(z^2+1)^{\kappa+1}}.$$

Thus the imaginary part of the dielectric permittivity is

$$\mathrm{Im}[\varepsilon_L] = \frac{2\Gamma(\kappa+1)z^3}{\Gamma(\kappa-1/2)r^2}\frac{\sqrt{\pi}}{(z^2+1)^{\kappa+1}}, \tag{17}$$

where $r=f/f_p=w/w_p$.

The first part of Eq. (16) will be numerically integrated taking care of the infinite upper and lower limits. Due to the term $1/(x-z)$, the integration needs to be separated in three parts,

$$\begin{aligned}\int_{-\infty}^{+\infty}\frac{1}{(x-z)}\left[\frac{1}{(x^2+1)^{\kappa+1}}-\frac{1}{(z^2+1)^{\kappa+1}}\right]dx \\ = \int_{-\infty}^{-\beta}\frac{1}{(x-z)}\left[\frac{1}{(x^2+1)^{\kappa+1}}-\frac{1}{(z^2+1)^{\kappa+1}}\right]dx \\ + \int_{-\beta}^{+\beta}\frac{1}{(x-z)}\left[\frac{1}{(x^2+1)^{\kappa+1}}-\frac{1}{(z^2+1)^{\kappa+1}}\right]dx \\ + \int_{+\beta}^{+\infty}\frac{1}{(x-z)}\left[\frac{1}{(x^2+1)^{\kappa+1}}-\frac{1}{(z^2+1)^{\kappa+1}}\right]dx, \end{aligned} \tag{18}$$

where $\beta>z$, so that

$$\begin{aligned}\frac{-1}{(z^2+1)^{\kappa+1}}\left(\int_{-\infty}^{-\beta}\frac{1}{(x-z)}dx+\int_{+\beta}^{+\infty}\frac{1}{(x-z)}dx\right) \\ = \frac{-1}{(z^2+1)^{\kappa+1}}\left[\ln\left(\frac{\beta+z}{\beta-z}\right)\right].\end{aligned}$$

The remaining parts are proper integrals which can be calculated numerically after using Taylor's expansion in l'Hôpital's rule around $x=z$. The longitudinal dielectric permittivity calculated by this method is valid for any values of kappa greater than 3/2. In the particular case when κ is integer, it is equivalent to the formula given by Ref. 7 and used in Refs. 11 and 20.

D. Kappa electron thermal noise

The fluctuations of the electrostatic field are given in Eq. (3). The dielectric function ε_L has just been calculated. $F(kL)$ depends on the geometry of the antenna with expression (6) or expression (7) for, respectively, wire or sphere antennas, where L is the length of the antenna. Let us now calculate $B(k)$.

Inserting Eq. (8) into Eq. (4), we get

$$B(k) = \frac{2\pi A}{k}\int_{\omega/k}^{+\infty}\frac{v}{(1+v^2/\kappa v_0^2)^{\kappa+1}}dv,$$

which gives, after we set $x=v^2/\kappa v_0^2$ and $z=\omega/\kappa^{1/2}kv_0$,

$$B(k) = \frac{\pi A v_0^2}{k}\frac{1}{(1+z^2)^{\kappa}}. \tag{19}$$

Substituting this expression of $B(k)$ into Eq. (3) and setting $r=\omega/\omega_p$, $u=L/L_D$ with L_D given by Eq. (11), v_0 given by Eq. (10), and A given by Eq. (9), we find the expression of the normalized QTN spectrum,

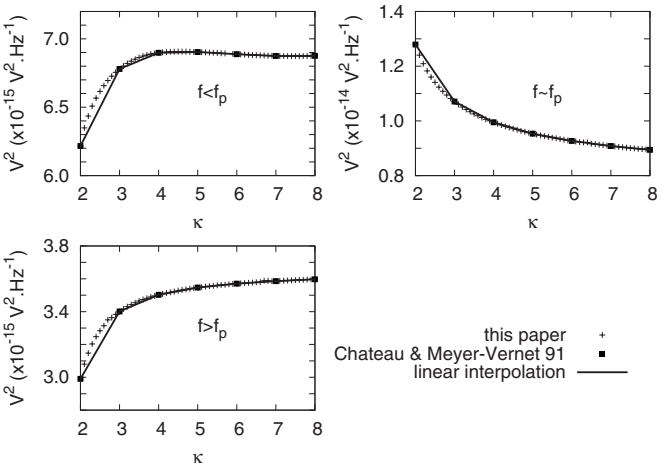

FIG. 1. Electron noise power level in $V^2\ Hz^{-1}$ as a function of κ between 2 and 8 calculated for a wire antenna with $l=35$ m, $n_e=4\times10^5$ m^{-3}, and $T_e=1.5\times10^5$ K for three frequencies such as $f<f_p$, $f\approx f_p$, and $f>f_p$. The cross symbols show our calculation for real values of κ and the black square symbols are calculated by the formula given by Chateau and Meyer-Vernet (Ref. 7) for integer values of κ. The lines are the linear interpolations between two close integer values of κ.

$$\frac{V^2}{T_e^{1/2}} = \frac{16}{\pi^{3/2}\varepsilon_0\kappa}\frac{1}{r^2}m_e^{1/2}k_B^{1/2}(2\kappa-3)^{1/2}\frac{\Gamma(\kappa+1)}{\Gamma(\kappa-1/2)} \times\int_0^{+\infty}F\left(\frac{ru}{z(2\kappa-1)^{1/2}}\right)\frac{zdz}{|\varepsilon_L|^2(1+z^2)^{\kappa}}. \tag{20}$$

Figure 1 shows that the calculations presented in this section agree with the results of Chateau and Meyer-Vernet[7] for integer values of κ. A linear interpolation between two integer values of κ may not be accurate enough to calculate V^2 with real values of κ, especially for $\kappa<3$.

III. OTHER CONTRIBUTIONS OF THE QUASI-THERMAL NOISE

A. Shot noise and antenna impedance

Since the antenna is a physical object which disturbs the trajectories of the particles (they cannot pass through its surface) and furthermore the antenna surface can eject photoelectrons, there is an additional noise, which will be called shot noise in this paper. In dilute space plasmas, the antenna radius a and dc potential ϕ often satisfy $a<L_D$ and $|e\phi/k_BT_e|<1$. Then, a good approximation for this shot noise[10] is given by

$$V_S^2 = 2e^2N_e|Z|^2, \tag{21}$$

where $N_e=(4\pi)^{-1/2}nv_{\mathrm{the}}S$ is the electron impact rate on one antenna arm[10] with $S=2\pi aL$ and $S=4\pi a^2$ for a wire and a sphere antenna, respectively.

The antenna impedance Z is given by

$$Z = \frac{4i}{\pi^2\varepsilon_0\omega}\int_0^{\infty}\frac{F(kL)F_a(ka)}{\varepsilon_L}dk, \tag{22}$$

with the function F given in Eq. (6) or Eq. (7), and F_a taking into account the finite radius a of the antenna as

$$F_a(x) = J_0^2(x) \quad \text{(wires)},$$

$$F_a(x) = \left(\frac{\sin x}{x}\right)^2 \quad \text{(spheres)},$$

where $J_0(x)$ is the Bessel's function.

The relative contribution of this noise V_S^2/V^2 for $f/f_p < 1$ is generally negligible for the wire dipole (since $a < L_D$), but it is dominant for sphere antennas.[10] This is the reason why QTN measurements on space missions used wire dipoles. For wire antennas, this noise decreases with frequency as $1/f^2$.

The antenna impedance (22) is the main contribution of the radio receiver impedance Z_R.[21] Hence the voltage power spectrum V_ω^2, which is the interesting quantity, is related to that measured by the receiver V_R^2 by the relation

$$V_R^2 = V_\omega^2 \left| \frac{Z_R}{Z_R + Z} \right|^2. \tag{23}$$

Thus, a good determination of the antenna impedance is required for any accurate plasma measurement.

B. Ion thermal noise in drifting plasma

In the case of a drifting plasma where the thermal velocity v_{thi} of the ion is smaller than the velocity of the plasma V, like the solar wind, the lower-frequency part of the QTN spectrum is due to the above-mentioned shot noise and to the ion thermal noise, which is Doppler shifted by the plasma velocity. This noise has been extensively studied in Ref. 3. The ion contribution to the voltage power spectrum in cylindrical coordinates of axis parallel to $\vec{V}$ is

$$V_i^2 = \frac{8}{\pi^{5/2}} \frac{ne^2}{\varepsilon_0^2} \frac{1}{v_{\text{thi}}} \int_0^{+\infty} \frac{dk}{k^3} \times \int_{-1}^{+1} \frac{\exp[(\omega - kVu)^2/v_{\text{thi}}^2 k^2]}{|\varepsilon_L(\vec{k}, \omega - kVu)|^2} du \times \int_0^{2\pi} \frac{\sin^4\left(\frac{kL}{2}\cos\gamma\right)}{(kL\cos\gamma)^2} d\psi, \tag{24}$$

where $u = \cos\theta$ with θ as the angle between $\vec{k}$ and $\vec{V}$, and γ is the angle between the antenna and $\vec{k}$ given by

$$\cos\gamma = u\cos\beta + \sqrt{1-u^2}\sin\beta\cos\psi,$$

where β is the angle between $\vec{V}$ and the antenna, and ψ is the azimuthal angle of $\vec{k}$ in a plane perpendicular to $\vec{V}$.

To deduce a simpler formula to be used for a plasma diagnostic, one could consider the two simple cases where the antenna is perpendicular or parallel to the velocity $\vec{V}$.[3] The first case is the most interesting in practice. Since the effect of the velocity is maximum for $\vec{k}$ parallel to $\vec{V}$ and since for a long antenna the maximum response is ultimately at 90° from the antenna direction,[22] the ion contribution to the thermal noise (which increases with the Doppler shift) is expected to be maximum when the antenna is perpendicular to $\vec{V}$.

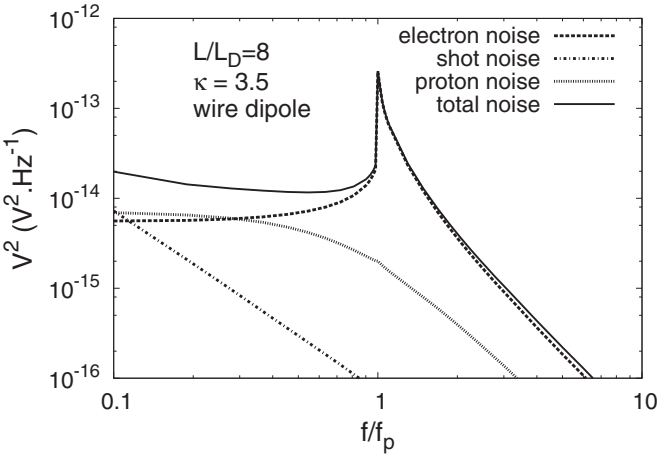

FIG. 2. A typical theoretical QTN spectrum with a kappa velocity distribution for the electrons (solid line) and the different contributions: the electron thermal noise (dashed line), the Doppler-shifted proton noise (dotted line) and the shot noise (dashed-dotted line) for a wire dipole antenna such as $L/L_D=8$ and $a=1.1$ cm with $\kappa=3.5$, $n=5.6\times10^6$ m^{-3}, $T_e=1.12\times10^5$ K, $T_p=2.7\times10^5$ K, and $V=800$ km s^{-1}.

Figure 2 represents a typical example of QTN spectrum in the solar wind (solid line) and its different contributions: the electron QTN considering kappa distribution with $\kappa=3.5$ (dashed line), the Doppler-shifted proton noise (dotted line), and the shot noise (dashed-dotted line) for a wire dipole antenna such as $L/L_D=8$ with $\kappa=3.5$, $n=5.6\times10^6$ m^{-3}, $T_e=1.12\times10^5$ K, $T_p=2.7\times10^5$ K, and $V=800$ km s^{-1}.

IV. RESULTS AND DISCUSSIONS

In this part, since the sphere antennas are not used in practice for QTN analysis, we will focus on the electron contribution of the QTN with a wire dipole antenna. The double sphere antenna case can be found in Ref. 7 for integer value of κ.

Figure 3 shows a set of normalized spectra calculated with a kappa distribution with $\kappa=3.5$ for different values of the normalized antenna length L/L_D. This illustrates the ge-

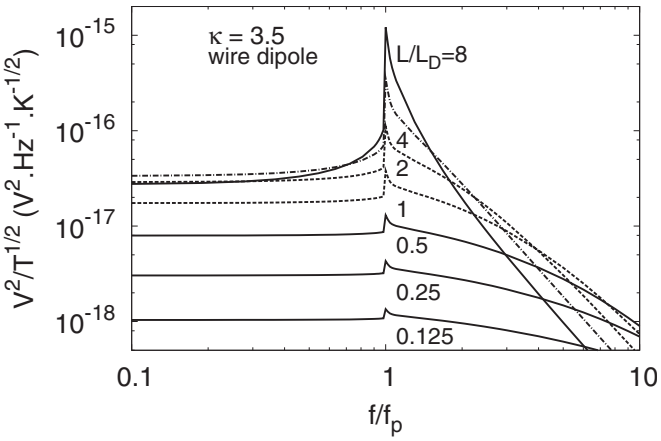

FIG. 3. Noise power spectrum in V^2 Hz^{-1} normalized to T_e(K)$^{1/2}$ calculated with a kappa electron distribution ($\kappa=3.5$) and a wire dipole antenna for different values of the normalized antenna length L/L_D.

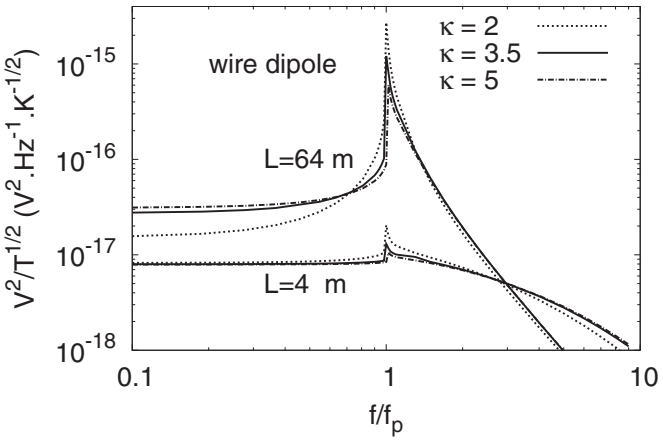

FIG. 4. Noise power spectrum in V^2 Hz^{-1} normalized to $T_e(K)^{1/2}$ calculated with a kappa electron distribution $\kappa=2,3.5,5$ and a wire dipole antenna with two different values of the antenna length. The antenna lengths $L=4$ and $L=64$ meters correspond to, respectively, 0.5 and 8 times the Debye length for $\kappa=3.5$, $n=5.6\times10^6$ m^{-3}, and $T_e=1.12\times10^5$ K.

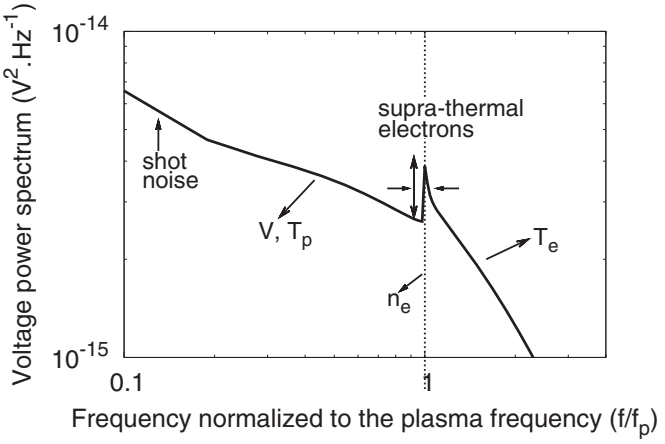

FIG. 5. A generic QTN spectrum with the different contributions obtained with $n_e=5.6\times10^6$ m^{-3}, $T_e=1.12\times10^5$ K, $\kappa=3.5$, $T_p=2.7\times10^5$ K, $V=800$ km s^{-1}, and a wire antenna such as $L=10$ m and $a=1.1\times10^{-3}$ m.

neric behavior of QTN spectra: a plateau below f_p, a cutoff at f_p with a peak, which is sharper for longer antennas, and a high-frequency spectrum proportional to f^{-3}. The spectrum is nearly flat for short antennas. For longer antennas, the peak is sharp and occurs at f_p, which allows a very precise measurement of n_e since the electron density is proportional to f_p^2.

Figure 4 shows the effect of changing the parameter κ for a wire dipole antenna with two different values of the antenna length, 4 and 64 m corresponding to, respectively, 0.5 and 8 times the Debye length for $\kappa=3.5$, $n=5.6\times10^6$ m^{-3}, and $T_e=1.12\times10^5$ K. Thus, the spectrum with $u=0.5$ and $u=8$ is equivalent in Figs. 3 and 4. The low-frequency level does not depend very much on κ for $\kappa\gg1$, especially for shorter antennas. This is because it depends mainly on the bulk of the velocity distribution.[9,10] The effect of varying κ is stronger close to the plasma frequency. We also see that for a long wire antenna the high-frequency level depends not on κ, but only on n and T_e. At frequency close to the plasma frequency, the phase velocity of Langmuir waves becomes very large, since the wave number is zero at f_p. Consequently, the fastest particles will resonate with these waves, producing the noise peak at $f\approx f_p$. Since the κ index is related to the proportion of suprathermal electrons, its high influence on the QTN spectrum at the plasma frequency is easily explained.

V. CONCLUSIONS

We developed the numerical solution for the determination of the longitudinal dielectric permittivity in the case of a kappa distribution function for all values of κ and applied it to the QTN spectroscopy. We derived the following properties of the electron QTN in this case. The κ parameter's main influence takes place close to the plasma frequency and above. The high-frequency ($f\gg f_p$) noise level on a wire antenna of length $L\gg L_D$ only depends on the electron density (n) and temperature (T_e), and the analytic expression

$$V^2(V^2\ Hz^{-1}) \approx 4\times10^{-11}T_e(K)n(m^{-3})/f^3(Hz)L(m)$$

given by Chateau and Meyer-Vernet[7] can be used to obtain an approximation of the noise level. Therefore the measurement of this level gives a direct determination of the pressure for any stable distribution function.

Figure 5 summarizes the parameters one could expect to determine with the QTN spectroscopy in a drifting and collisionless plasma, like the solar wind. In a more practical view, the calculation of the QTN with any value of the parameter κ allows us to analyze the data provided by space missions in order to obtain precise measurements of the electron density, temperature, and nonthermal parameters in the solar wind, which is essential to understand the energy transport in collisionless plasma.

[1] N. Rostoker, Nucl. Fusion **1**, 101 (1961).
[2] N. Meyer-Vernet, S. Hoang, K. Issautier, M. Maksimovic, R. Manning, M. Moncuquet, and R. G. Stone, *Measurement Techniques in Space Plasmas: Fields*, Geophysical Monograph No. 103 (AGU, Washington, D.C., 1998), p. 205.
[3] K. Issautier, N. Meyer-Vernet, M. Moncuquet, S. Hoang, and D. J. McComas, J. Geophys. Res. **104**, 6691, doi:10.1029/1998JA900165 (1999).
[4] M. Maksimovic, I. Zouganelis, J. Chaufray, K. Issautier, E. E. Scime, J. E. Littleton, E. Marsch, D. J. McComas, C. Salem, R. P. Lin, and H. Elliott, J. Geophys. Res. **110**, A09104, doi:10.1029/2005JA011119 (2005).
[5] V. M. Vasyliunas, J. Geophys. Res. **73**, 2839, doi:10.1029/JA073i009p02839 (1968).
[6] S. Olbert, *Physics of the Magnetosphere*, Astrophysics and Space Science Library Vol. 10, edited by R. D. Carovillano, J. F. McClay, and H. R. Radoski (Springer, Berlin, 1968), p. 641.
[7] Y. F. Chateau and N. Meyer-Vernet, J. Geophys. Res. **96**, 5825, doi:10.1029/90JA02565 (1991).
[8] A. G. Sitenko, *Electromagnetic Fluctuations in Plasma* (Academic, New York, 1967).
[9] Y. F. Chateau and N. Meyer-Vernet, J. Geophys. Res. **94**, 15407, doi:10.1029/JA094iA11p15407 (1989).
[10] N. Meyer-Vernet and C. Perche, J. Geophys. Res. **94**, 2405, doi:10.1029/JA094iA03p02405 (1989).
[11] I. Zouganelis, J. Geophys. Res. **113**, A08111, doi:10.1029/2007JA012979 (2008).
[12] F. Valentini and R. D'Agosta, Phys. Plasmas **14**, 092111 (2007).
[13] R. Silva, A. R. Plastino, and J. A. S. Lima, Phys. Lett. A **249**, 401 (1998).
[14] M. P. Leubner, Astrophys. Space Sci. **282**, 573 (2002).
[15] J. A. S. Lima, R. Silva, and A. R. Plastino, Phys. Rev. Lett. **86**, 2938 (2001).

[16]F. M. Ramos, R. R. Rosa, and L. A. W. Bambace, Physica A **344**, 626 (2004).
[17]A. R. Plastino, C. Giordano, A. Plastino, and M. Casas, Physica A **336**, 376 (2004).
[18]C. Tsallis, J. Stat. Phys. **52**, 479 (1988).
[19]B. D. Shizgal, Astrophys. Space Sci. **312**, 227 (2007).
[20]I. Zouganelis, M. Maksimovic, N. Meyer-Vernet, S. D. Bale, J. P. Eastwood, A. Zaslavsky, M. Dekkali, K. Goetz, and M. L. Kaiser, "Measurements of stray antenna capacitance in the STEREO/WAVES instrument: Comparison of the measured voltage spectrum with an antenna electron shot noise model," Radio Sci. (in press).
[21]N. Meyer-Vernet, S. Hoang, K. Issautier, M. Moncuquet, and G. Marcos, *Radio Astronomy at Long Wavelengths*, Geophysical Monograph No. 119 (AGU, Washington, D.C., 2000), p. 67.
[22]N. Meyer-Vernet, Geophys. Res. Lett. **21**, 397, doi:10.1029/94GL00197 (1994).